Journal of Nuclear Medicine, published on March 12, 2021 as doi:10.2967/jnumed.120.260141

Quantitation of Post-Stress Change in Ventricular Morphology Improves Risk Stratification

Robert JH Miller, MD[1,2], Tali Sharir, MD[3], Yuka Otaki, MD, PhD[2], Heidi Gransar, MS[2], Joanna X Liang, BA[2], Andrew J Einstein, MD, PhD[4], Mathews B Fish, MD[5], Terrence D. Ruddy, MD[6], Philipp A Kaufmann, MD[7], Albert J Sinusas, MD[8], Edward J Miller, MD, PhD[8], Timothy M Bateman, MD[9], Sharmila Dorbala, MD, MPH[10], Marcelo Di Carli, MD[10], Balaji K Tamarappoo, MD PhD[2], Damini Dey, PhD[2], Daniel S Berman, MD[2], Piotr J Slomka, PhD[2]

1. Department of Cardiac Sciences, University of Calgary, Calgary AB, Canada
2. Department of Imaging, Medicine, and Biomedical Sciences, Cedars-Sinai Medical Center, Los Angeles CA United States
3. Department of Nuclear Cardiology, Assuta Medical Center, Tel Aviv Israel
4. Division of Cardiology, Department of Medicine, and Department of Radiology, Columbia University Irving Medical Center, New York NY United States
5. Oregon Heart and Vascular Institute, Sacred Heart Medical Center, Springfield OR United States
6. Division of Cardiology, University of Ottawa Heart Institute, Ottawa ON Canada
7. Department of Nuclear Medicine, Cardiac Imaging, University Hospital Zurich, Zurich Switzerland
8. Section of Cardiovascular Medicine, Department of Internal Medicine, Yale University, New Haven CT United States
9. Cardiovascular Imaging Technologies LLC Kansas City MO United States
10. Division of Nuclear Medicine and Molecular Imaging, Department of Radiology, Brigham and Women's Hospital Boston MA United States

Brief title: Prognostic Use of Ventricular Morphology

Total word count: 5867 (including all elements)

Corresponding Author:

Piotr Slomka, PhD, FACC
Cedars-Sinai Medical Center
8700 Beverly Boulevard, Ste. A047N
Los Angeles, California 90048
Phone: 310-423-4348
Fax: 310-423-0173
Email: slomkap@cshs.org

First Author
Robert JH Miller, MD, FRCPC, FACC
University of Calgary

GAA 08, HRIC
3230 Hospital Drive NW
Calgary, AB, T2N 4Z6
Phone: 403-220-8191
Fax: 403-210-9350
Email: Robert.miller@ahs.ca

ABSTRACT (241/350 words)

Shape index and eccentricity index are measures of left ventricular morphology. Although both measures can be quantified with any stress imaging modality, they are not routinely evaluated during clinical interpretation. We assessed their independent associations with major adverse cardiovascular events (MACE), including measures of post-stress change in shape index and eccentricity index.

Methods:

Patients undergoing single photon emission computed tomography (SPECT) myocardial perfusion imaging (MPI) between 2009 and 2014 from the REFINE SPECT registry were studied. Shape index (ratio between the maximum LV diameter in short axis and ventricular length) and eccentricity index (calculated from orthogonal diameters in short axis and length) were calculated in end-diastole at stress and rest. Multivariable analysis was performed to assess independent associations with MACE (death, non-fatal myocardial infarction, unstable angina, or late revascularization).

Results:

In total, 14,016 patients, mean age 64.3 ± 12.2 and 8469 (60.4%) male, were included. MACE occurred in 2120 patients during a median follow-up of 4.3 years (interquartile range 3.4 – 5.7). Rest, stress, and post-stress change in shape and eccentricity indices were associated with MACE in unadjusted analyses (all $p<0.001$). However, in multivariable models only post-stress change in shape index (adjusted HR 1.38, $p<0.001$) and eccentricity index (adjusted HR 0.80, $p=0.033$) remained associated with MACE.

Conclusions:

Two novel measures, post-stress change in shape index and eccentricity index, were independently associated with MACE and improved risk estimation. Changes in ventricular morphology have important prognostic utility and should be included in patient risk estimation following SPECT MPI.

KEYWORDS: SPECT; myocardial perfusion; ventricular morphology; shape index; eccentricity index

INTRODUCTION

Stress myocardial perfusion imaging (MPI) with single photon emission computed tomography (SPECT), echocardiography or cardiovascular magnetic resonance imaging can provide full three-dimensional analysis of the left ventricle, providing information regarding ventricular remodeling in addition to assessing perfusion. Shape index, defined as the ratio of the maximum left ventricular (LV) dimension in short axis to the LV length, has been associated with increased risk of heart failure hospitalization(*1*). Eccentricity index is an additional marker of LV remodeling which is highly correlated with ventricular function(*2*). Sphericity index is a related concept which has been described for echocardiography(*3*) and cardiovascular magnetic resonance(*4*). While there is strong evidence regarding the prognostic significance of left ventricular remodeling pattern(*5*), the additive prognostic value of shape index and eccentricity index have not been tested in a large population with adjustment for important confounders. Additionally, the prognostic utility of change in these variables between stress and rest has not been described.

In the largest study to date, we assessed the independent prognostic significance of shape index and eccentricity index including measures of change in these parameters.

MATERIALS AND METHODS

Study Population

The multi-center, international REgistry of Fast Myocardial Perfusion Imaging with NExt generation SPECT (REFINE SPECT) includes patients who have undergone SPECT MPI with solid-state camera systems. The full details of the structure of the registry, image acquisition and analysis, and quality control have been previously described(*6*). We analyzed 20,418 consecutive patients enrolled in the REFINE SPECT registry between 2008 and 2014. Patients

without stress and rest ^{99m}Tc gated supine acquisitions were excluded (n=5803). Patients who underwent early revascularization, defined as percutaneous coronary intervention or coronary artery bypass grafting within 90 days of SPECT (n=599), were also excluded since this may have impacted long-term clinical outcomes(*7*). In total, 14,016 patients were included in the analysis. The study was approved by the institutional review boards at each participating institution and the overall study was approved by the institutional review board at Cedars-Sinai Medical Center. All data were collected under the NIH sponsored REFINE SPECT registry.

Clinical Data

Demographic information included: age, gender, body mass index, family history of coronary artery disease (CAD), smoking status, history of previous myocardial infarction (MI), previous revascularization, hypertension, diabetes, and dyslipidemia. Patients underwent exercise stress (n=5744), pharmacologic stress (n=7526 including: n=1304 adenosine, n=1381 regadenoson, n=40 dobutamine, and n=4801 dipyridamole) or pharmacologic stress with low-level exercise (n=746 total, n=38 dipyridamole walk and n=708 regadenoson walk).

Image Acquisition and Interpretation

Five centers participated in the prognostic arm of the REFINE SPECT registry. Three sites used a D-SPECT camera (Spectrum-Dynamics, Caesarea, Israel) while the other sites used Discovery NM 530c or NM/CT570c systems (GE Healthcare, Haifa, Israel). Imaging protocols included one day rest-stress (n=8729, 62.3%), one day stress-rest (n=5135, 36.5%), two day stress-rest (n=168, 1.2%) using site-specific protocols. Sites used either ^{99m}Tc-tetrofosmin or ^{99m}Tc-sestamibi radiotracers. Weight-adjusted mean doses were used: one day rest-stress (rest dose 260±94 MBq [7.0±2.5mCi], stress dose 966 ± 419 MBq [26.1±11.3mCi]), one day stress-rest (rest dose 821 ± 182 MBq [22.2±4.9mCi], stress dose 293 ± 78 MBq [7.9±2.1mCi]) and two

day stress-rest (rest dose 596 ± 556 MBq [16.1±15.0mCi], stress dose 814 ± 431 MBq [22.0±11.6mCi]). The cohort mean effective dose was 7.9 mSv. Upright (D-SPECT) and supine (Discovery NM 530c/570c) stress images were acquired 15-30 minutes after exercise stress and 30-60 minutes after pharmacologic stress over a total of 4-6 minutes(*6*). Additional stress imaging in either supine (D-SPECT) or prone (Discovery scanners) position was performed immediately afterwards. Resting image acquisition was performed with 6 to 10-minute acquisition times.

De-identified image datasets were transferred to the core laboratory (Cedars-Sinai Medical Center) where automated quantitation was performed by experienced technologists(*6*). Myocardial contours were generated automatically with Quantitative Perfusion SPECT/Quantitative Gated SPECT software (Cedars-Sinai Medical Center, Los Angeles, CA). Myocardial perfusion was quantified by total perfusion deficit (TPD) which incorporates severity and extent of perfusion abnormalities and is more reproducible compared to visual ischemia scoring(*8,9*). Left ventricular ejection fraction (LVEF) was assessed on the supine resting study with reduced defined as <40%. Phase SD, a measure of ventricular dyssynchrony, was calculated automatically at rest and stress. TID was calculated as the ratio between left ventricular volume at stress compared to rest on ungated acquisitions, using previously established thresholds for abnormal(*10*).

Left bundle branch block was present in 679 (4.8%) patients but would not be expected to influence measurement of eccentricity index or shape index. There was no interaction between the presence of left bundle branch block and the associations between post-stress change in shape index (interaction p=0.377) or post-stress change in eccentricity (interaction p=0.632) with major

adverse cardiovascular events (MACE). Shape index and eccentricity index have previously been demonstrated to have excellent repeatability (r^2=0.85 and 0.99, respectively)(*1,2*).

For the calculation of shape index, first the maximum diameter of the LV is found across all short-axis slices from the endocardial surface of the 3-dimensional contours. Next, the maximal length is determined as the distance between the most apical point on the endocardial surface to the center of the valve plane. Shape index was calculated as the ratio of the maximum LV diameter in short axis, across all short axis slices, to the ventricular length from the endocardial surface at end-diastole(*1*). Shape index was quantified on stress and rest scans and expressed as a percentage. Thus, a shape index value of 100% represents a maximum short axis diameter for the LV which is equal the long axis LV diameter. Post-stress change in shape index was calculated as stress minus rest shape index. Eccentricity index was measured from the mid-myocardial surface from a fitted ellipsoid using the diameters in short axis (x and y) and length (z). End-diastolic eccentricity index, calculated as $(1- (xy/z^2))^{0.5}$, was quantified automatically during image processing for rest and stress acquisitions and expressed as a percent(*2*). Thus for eccentricity index a value 0% represents a perfect sphere. Post-stress change in eccentricity index was calculated as stress minus rest eccentricity index. Importantly, eccentricity index is calculated from a 3-dimensional ellipsoid fitted to the entire LV, while shape index represents the most abnormal short axis dimension for the LV without any geometric assumptions (by assessing all possible short-axis slices). Graphical comparison of the concepts of shape index and eccentricity index, with two patient examples, are shown in Figure 1**.** All measures were attained automatically at the core laboratory and are calculated from gated images at end-diastole.

Outcomes

Patients were followed for development of MACE which includes all-cause mortality, non-fatal MI, hospitalization for unstable angina, and late revascularization. Unstable angina was defined as recent onset or escalating cardiac chest pain with negative cardiac biomarkers. All outcomes were adjudicated by cardiologists after considering all available investigations. In a secondary analysis, we considered only all-cause mortality. Additional details regarding event definitions and ascertainment have been previously reported(*6*).

Statistical Analysis

Univariable and multivariable Cox proportional hazards analysis was performed to assess associations with MACE using a multivariable model based on previous work(*11*). Stress shape index and stress eccentricity index were not included in the multivariable model due to the inclusion of both rest and post-stress change in values. Rest and post-stress change in shape index and eccentricity index were used to be consistent with the typical clinical framework of reporting fixed and ischemic perfusion defects. The analysis was repeated with a non-parsimonious model. The proportional hazard assumption was assessed with Schoenfeld residuals and was valid in all models. Collinearity in the model was assessed with a correlation matrix, with significant correlation identified between rest eccentricity index and rest shape index (r=0.830). No other significant correlation was identified. Interactions were assessed between shape index and eccentricity index with all other variables in the model, with significance assessed after a Bonferroni correction. There was no interaction between stress LVEF, rest LVEF, change in LVEF, reduced LVEF, or LV volume and rest shape index, post-stress change in shape index, rest eccentricity index or post-stress change in eccentricity index. Additionally, in patients undergoing pharmacologic stress there were no significant interactions

between pharmacologic stress agent or the use of adjunctive low-level exercise and rest or post-stress change in shape index or eccentricity index (all $p>0.1$).

When evaluating the independent prognostic utility of shape index and eccentricity index variables, each variable was assessed separately with the remaining variables (not shape index or eccentricity index) from the multivariable model. Net re-classification index (NRI) was used to assess the additive prognostic utility of shape index and eccentricity index variables.

Receiver operating characteristic (ROC) curves for discrimination of MACE during the entire follow-up period were also generated for each variable and areas under the curve (AUC) was compared using the method of Delong et al(*12*). Cut-off values were established using the Youden index for the overall population. To further assess post-stress change in shape index, a one-site-left-out approach was also performed in which each site was sequentially held out from ROC construction in order to assess variability in the optimal cut-off and provide repeated external validation of the optimal cut-off.

All statistical tests were two-sided, with a p-value < 0.05 considered significant. All analyses were performed using Stata version 13 (StataCorp, College Station, Texas). The study was approved by the institutional review boards at each participating institution and the overall study was approved by the institutional review board at Cedars-Sinai Medical Center. All data were collected under the NIH sponsored REFINE SPECT registry.

Subgroup Analyses

Unadjusted and adjusted associations between shape index and eccentricity index were assessed in patients undergoing exercise and pharmacologic stress separately. Similarly, associations were assessed in patients with and without reduced LVEF (defined as LVEF <40%). Lastly, we assessed the associations between stress shape index and stress eccentricity index in

an expanded population including those undergoing stress-only imaging, with results in the supplement.

RESULTS

Population Characteristics

In total 14,016 patients with mean age 64.3 ± 12.2 years and 8,469 (60.4%) males were included. Baseline population characteristics are outlined in Table 1. Patients who experienced MACE were older (mean age 69.4 vs 63.3 years, $p<0.001$) and more likely to have diabetes (38.2% vs. 23.3%, $p<0.001$) and undergo pharmacologic stress (75.3% vs. 56.1%, $p<0.001$).

Imaging characteristics are shown in Table 2. Rest, stress, and post-stress change in shape index were all significantly higher in patients who experienced MACE ($p<0.001$ for all). Rest, stress, and post-stress change in eccentricity index were all lower in patients who experienced MACE ($p<0.001$ for all). Stress TPD (mean 8.2 vs. 4.3, $p<0.001$) and the prevalence of reduced LVEF (11.8% vs. 4.1%, $p<0.001$) were also higher in patients who experienced MACE. Imaging characteristics stratified by mode of stress as shown in Supplemental Table 1**.** There were significant differences in all shape index and eccentricity index variables between exercise and pharmacologic stress.

Outcomes

MACE occurred in 2,120 patients during a median follow-up of 4.3 years (interquartile range 3.4 – 5.7). MACE included 1,098 (7.8%) deaths, 966 (6.9%) revascularizations, 287 (2.1%) MI, and 180 (2.0%) admissions for unstable angina.

Event rates across deciles of post-stress change in shape index are shown in Figure 2. There was an increase in annualized MACE rates with increasing decile of post-stress change in

shape index, ranging from 1.6% in the lowest decile to 5.2% in the highest decile. Event rates across deciles of delta eccentricity index are shown in Figure 3. Increasing post-stress change in eccentricity index was associated with a decrease in annualized MACE rates, ranging from 5.0% in the lowest decile to 2.1% in the highest decile. Figure 4 shows Kaplan-Meier survival curves for shape index and eccentricity index.

Associations with MACE

The results of univariable and multivariable analyses are outlined in Table 3**.** Rest, stress, and post-stress change in shape index and eccentricity index were all significantly associated with MACE in unadjusted analyses (all $p<0.001$). However, in multivariable models only delta shape index (adjusted HR 1.38 per 10% change, 95% CI 1.20 – 1.58, $p<0.001$) and post-stress change in eccentricity index (adjusted HR 0.80 per 10% change, 95% CI 0.0.66 – 0.98, $p=0.033$) remained associated with MACE. Although stress shape index and stress eccentricity index were not included in the multivariable model, both were significant when used in place of post-stress change in values (adjusted HR 1.38, 95% CI 1.17 – 1.54, $p<0.001$ and adjusted HR 0.80, 95% CI 0.66 – 0.98, $p=0.035$ respectively). Results were similar in the non-parsimonious multivariable analysis (Supplemental Table 2**).**

Variable Correlation

Correlation between shape index and eccentricity index variables with each other as well as with LVEF, TID, and phase SD are shown in Supplemental Figures 1 to 4. There was significant, but poor, correlation between ischemic TPD and post-stress change in shape index ($r^2=0.133$, $p<0.001$) and eccentricity index ($r=-0.100$, $p<0.001$). There was poor correlation between stress and post-stress change in eccentricity index and shape index with peak stress BP or peak stress HR (all $r^2<0.100$).

Test Characteristics

Summary of NRI for MACE with the addition of shape index and eccentricity index variables to the remainder of the multivariable model are outlined in Supplemental Table 3. Post-stress change in shape index and post-stress change in eccentricity index were associated with the highest continuous NRI.

AUC for shape index and eccentricity index as single parameters are shown in Supplemental Figure 5. Of the shape index and eccentricity index variables, post-stress change in shape index had the highest discrimination of MACE during follow-up (AUC 0.597, 95%CI 0.584 – 0.610), followed by stress shape index (AUC 0.580) and post-stress change in eccentricity index (AUC 0.571). In comparison, the AUC for ischemic TPD was 0.643 (95% CI 0.630 – 0.655) and for resting LVEF was 0.579 (95% CI 0.565 - 0.593).

Cut-off values, with associated annualized MACE rates, positive predictive value, and negative predictive values, derived in the overall population are shown in Supplemental Table 4. Summary of the cut-off values for post-stress change in shape index generated in the leave-one-site-out analysis are shown in Supplemental Table 5**.**

Sensitivity Analyses

The results of univariable and multivariable analysis of associations with all-cause mortality are in Supplemental Table 6. Associations stratified by mode of stress, presence of reduced LVEF (defined as LVEF <40%), and camera type are in Supplemental Table 7 to 9.

Expanded Stress Imaging Population

In order to more fully assess the potential clinical utility of measuring stress eccentricity index and stress shape index, we included a population of patients who underwent stress only imaging, with supine gated acquisitions and who did not undergo revascularization with

percutaneous coronary intervention or coronary artery bypass grafting within 90 days of SPECT MPI. In total, 2,731 patients were added bringing the total population to 16,747 patients.

MACE occurred in 2,300 (13.7%) patients during median follow-up of 4.2 years (IQR 3.5 – 5.2 years). After adjusting for the same variables as outlined in Table 3 (with the exception of stress TPD substituted for rest and ischemic TPD and stress LVEF substituted for rest LVEF), stress shape index was associated with MACE (adjusted HR 1.16, 95% CI 1.04 – 1.28, p=0.006) but stress eccentricity index was not (adjusted HR 0.98, 95% CI 0.83 – 1.17, p=0.856). Stress eccentricity was also not associated with MACE in the original patient population using the multivariable model with only stress imaging variables (adjusted HR 0.99, 95% CI 0.83 – 1.18, p=0.888).

DISCUSSION

We assessed the independent prognostic significance of shape index and eccentricity index after correcting for important confounding factors including LVEF and LV volumes. To our knowledge, this is the first study to describe post-stress change in shape index and post-stress change in eccentricity index as risk markers following stress MPI. We identified a graded change in MACE rates across deciles of shape index and eccentricity index. Additionally, after multivariable adjustment we found that post-stress change in shape index and post-stress change in eccentricity index were independently associated with increased MACE and significantly improved patient risk classification. Changes in ventricular morphology have important prognostic utility and should be included in patient risk estimation following SPECT MPI.

Our findings are consistent with previous studies outlining the prognostic significance of LV morphology and remodeling patterns. Abidov et al. demonstrated that higher stress shape

index was associated with an increased incidence of heart failure hospitalizations in 297 patients(*1*). In the Multi-Ethnic Study of Atherosclerosis, increased sphericity on cardiac magnetic resonance imaging was associated with incident heart failure and atrial fibrillation(*13*). Gimelli et al. demonstrated that eccentricity index is correlated with LVEF and LV volume in 456 patients(*2*), and was associated with significant CAD(*14*). We have expanded on this data by demonstrating that post-stress change in shape index and eccentricity index, quantified automatically, were associated with MACE in a substantially larger, multicenter, international population. Importantly, the associations between post-stress change in shape index and eccentricity index with MACE remained after adjusting for important confounders. Both measures also demonstrated significant improvements by NRI, suggesting that incorporation of post-stress change in ventricular morphology can improve risk stratification.

An important novel aspect of our work was assessment of rest, stress and change in ventricular morphology. In the multivariable model, post-stress change in shape index and eccentricity were more strongly associated with MACE than rest or stress values. Since all values were quantified automatically in our study, assessing changes in shape index and eccentricity could potentially improve risk stratification without increasing interpretation time. The correlation between post-stress change in shape index and eccentricity index was relatively poor. Therefore, it seems reasonable to consider changes in both parameters within the same risk model. All of these parameters could be efficiently combined using machine-learning based models(*15*). Alternatively, abnormal cut-offs could be employed by physicians similar to the current clinical approach to integrating TID. For example, patients in the 95th percentile for post-stress change in shape index and eccentricity index had a 50% increased risk of MACE.

Importantly, the thresholds for abnormal post-stress change in shape index demonstrated minimal variation using a one-site-left-out approach, suggesting broad generalizability.

While there is robust data supporting the prognostic utility of myocardial perfusion(*16*), non-perfusion markers can help identify patients with high-risk CAD including transient ischemic dilation (TID)(*17*), post-stress wall motion abnormalities(*18*), and reduced LVEF(*19*). These parameters are particularly important since a significant proportion of patients with multi-vessel CAD have normal relative, regional perfusion(*20*). Post-stress change in shape index and eccentricity index are additional markers which help identify these high-risk patients. Notably, stress shape index and stress eccentricity index were associated with MACE in the overall population, but only stress shape index remained associated in an expanded population including patients undergoing stress-only imaging and when considering only stress imaging variables.

The terminology used to describe findings of ventricular morphology has been variable. We used the term shape index to be consistent with existing SPECT MPI literature (*11*), but sphericity has been used to refer to the same ratio(*4,21*). However, other studies use the term sphericity to describe a volume/length ratio(*13,22*). Eccentricity index and shape index are related concepts to sphericity. Eccentricity index represents a 3-dimensional structure, while shape index represents a worst-case scenario 2-dimensional structure. Our study does not clarify the underlying pathophysiology behind these changes; however, the correlation with LVEF, TID ratio, phase SD, and TPD were all poor. The mechanism may relate to diffuse myocardial ischemia or cavity dilation similar to TID(*11*). Previous studies have shown that LVEF improves with exercise in patients without significant CAD, but may decrease in patients with significant CAD presumably related to ischemia(*23*). Similarly, myocardial hyperemia caused by pharmacologic stress can increase myocardial contractility(*24*). This effect, combined with

reduced systemic vascular resistance, leads to increased LVEF(*25*). While dipyridamole-induced myocardial dysfunction is associated with reduced subendocardial flow reserve(*26*). Global or regional ventricular dysfunction could lead to changes in ventricular loading conditions, leading to changes in shape index or eccentricity index. Differences in stress shape index and eccentricity variables between patients undergoing exercise and pharmacologic stress may reflect differences in these mechanisms. However, differences in resting values suggest that population characteristics also contribute to differences in these parameters. Additionally, differences in the prognostic significance of shape index and eccentricity index in exercise and pharmacologic stress populations should be interpreted cautiously since interaction testing was not significant, suggesting that the associated risks do not differ significantly. Dedicated studies are warranted to better define the mechanisms of these changes in ventricular morphology.

Our study has a few limitations. Imaging was performed in accordance with American Society of Nuclear Cardiology guidelines, with post-stress imaging occurring with a delay of 15-60 minutes(*27*). Earlier post-stress imaging may identify more substantial changes in shape index or eccentricity index. For example, early post-stress LVEF reserve can be used to identify patients with extensive CAD on positron emission tomography(*25*), and significant associations with MACE have been demonstrated with early, but not late, LVEF reserve on SPECT(*28*). We included several combinations of camera system and stress protocol which impact calculation of shape index and eccentricity index. However, thresholds for abnormal post-stress change in shape index were similar across sites suggesting that our results are generalizable. All images were acquired with solid-state cameras, so it is unclear to what extent our observations extend to conventional camera systems. However, Abidov et al. previously demonstrated that stress shape index was associated with heart failure hospitalizations in patients imaged with an Anger camera system in a smaller cohort(*1)*. Additionally, all-cause mortality was collected in this large multi-center registry

and different associations may be present with cardiac mortality. Lastly, prospective studies are required to determine whether incorporating shape index or eccentricity index during risk estimation improves patient outcomes.

CONCLUSIONS

This is the first study to describe post-stress change in shape index and post-stress change in eccentricity index as automated, quantitative measures of change in ventricular morphology. Post-stress change in shape index and eccentricity index were independently associated with MACE and improved risk estimation. Changes in ventricular morphology have important prognostic utility and should be included in patient risk estimation following SPECT MPI.

ACKNOWLEDGEMENTS

None.

FUNDING: This research was supported in part by grant R01HL089765 from the National Heart, Lung, and Blood Institute/ National Institutes of Health (NHLBI/NIH) (PI: Piotr Slomka). The content is solely the responsibility of the authors and does not necessarily represent the official views of the National Institutes of Health. The work was also supported in part by the Dr. Miriam and Sheldon Adelson Medical Research Foundation.

DISCLOSURES: Drs. Berman and Slomka participate in software royalties for QPS software at Cedars-Sinai Medical Center. Dr. Slomka has received research grant support from Siemens Medical Systems. Drs. Berman, Dorbala, Einstein, and Edward Miller have served as consultants

for GE Healthcare. Dr. Einstein has served as a consultant to W. L. Gore & Associates. Dr. Dorbala has served as a consultant to Bracco Diagnostics; her institution has received grant support from Astellas. Dr. Di Carli has received research grant support from Spectrum Dynamics and consulting honoraria from Sanofi and GE Healthcare. Dr. Ruddy has received research grant support from GE Healthcare and Advanced Accelerator Applications. Dr. Einstein's institution has received research support from GE Healthcare, Philips Healthcare, Toshiba America Medical Systems, Roche Medical Systems, and W. L. Gore & Associates. No other potential conflicts of interest relevant to this article exist.

KEY POINTS

Question: What is the independent prognostic significance of shape index and eccentricity index, measures of ventricular morphology, in patients undergoing SPECT MPI.

Pertinent Findings: In this retrospective analysis of a large, multicenter, international registry, post-stress change in shape index and eccentricity index were independently associated with MACE and improved risk estimation.

Implications for Patient Care: Changes in ventricular morphology have important prognostic utility and should be included in patient risk estimation following SPECT MPI.

REFERENCES

1. Abidov A, Slomka PJ, Nishina H, et al. Left ventricular shape index assessed by gated stress myocardial perfusion SPECT: initial description of a new variable. *J Nucl Cardiol.* 2006;13:652-659.

2. Gimelli A, Liga R, Clemente A, Marras G, Kusch A, Marzullo P. Left ventricular eccentricity index measured with SPECT myocardial perfusion imaging: An additional parameter of adverse cardiac remodeling. *J Nucl Cardiol.* 2020;27:71-79.

3. Medvedofsky D, Maffessanti F, Weinert L, et al. 2D and 3D echocardiography-derived indices of left ventricular function and shape: relationship with mortality. *JACC Cardiovasc Imaging.* 2018;11:1569-1579.

4. Halima AB, Zidi A. The cardiac magnetic resonance sphericity index in the dilated cardiomyopathy: New diagnostic and prognostic marker. *Archives of Cardiovascular Diseases Supplements.* 2018;10:42.

5. Verma A, Meris A, Skali H, et al. Prognostic implications of left ventricular mass and geometry following myocardial infarction. *JACC Cardiovasc Imaging.* 2008;1:582-591.

6. Slomka PJ, Betancur J, Liang JX, et al. Rationale and design of the REgistry of Fast Myocardial Perfusion Imaging with NExt generation SPECT (REFINE SPECT). *J Nucl Cardiol.* 2020;27:1010-1021.

7. Azadani PN, Miller RJH, Sharir T, et al. Impact of early revascularization on major adverse cardiovascular events in relation to automatically quantified ischemia. *JACC Cardiovasc Imaging.* 2020:3515.

8. Berman DS, Kang XP, Gransar H, et al. Quantitative assessment of myocardial perfusion abnormality on SPECT myocardial perfusion imaging is more reproducible than expert visual analysis. *J Nucl Cardiol.* 2009;16:45-53.

9. Xu Y, Fish M, Gerlach J, et al. Combined quantitative analysis of attenuation corrected and non-corrected myocardial perfusion SPECT. *J Nucl Cardiol.* 2010;17:591-599.

10. Hu L-H, Sharir T, Miller RJH, et al. Upper reference limits of transient ischemic dilation ratio for different protocols on new-generation cadmium zinc telluride cameras. *J Nucl Cardiol.* 2019;27:1180-1189.

11. Abidov A, Bax JJ, Hayes SW, et al. Transient ischemic dilation ratio of the left ventricle is a significant predictor of future cardiac events in patients with otherwise normal myocardial perfusion SPECT. *J Am Coll Cardiol.* 2003;42:1818-1825.

12. DeLong ER, DeLong DM, Clarke-Pearson DL. Comparing the areas under two or more correlated receiver operating characteristic curves. *Biometrics.* 1988;44:837-845.

13. Ambale-Venkatesh B, Yoneyama K, Sharma RK, et al. Left ventricular shape predicts different types of cardiovascular events in the general population. *Heart.* 2017;103:499-507.

14. Gimelli A, Liga R, Giorgetti A, Casagranda M, Marzullo P. Stress-induced alteration of left ventricular eccentricity. *J Nucl Cardiol.* 2019;26:227-232.

15. Hu LH, Miller RJH, Sharir T, et al. Prognostically safe stress-only single-photon emission computed tomography myocardial perfusion imaging guided by machine learning. *Eur Heart J Cardiovasc Imaging.* 2020;Epub ahead of print.

16. Otaki Y, Betancur J, Sharir T, et al. 5-Year prognostic value of quantitative versus visual mpi in subtle perfusion defects. *JACC Cardiovasc Imaging.* 2020;13:774-785.

17. Miller RJH, Hu LH, Gransar H, et al. Transient ischaemic dilation and post-stress wall motion abnormality increase risk in patients with less than moderate ischaemia. *Eur Heart J Cardiovasc Imaging.* 2020;21:567-575.

18. Sharir T, Bacher-Stier C, Dhar S, et al. Identification of severe and extensive coronary artery disease by postexercise regional wall motion abnormalities in Tc-99m sestamibi gated single-photon emission computed tomography. *Am J Cardiol.* 2000;86:1171-1175.

19. Sharir T, Germano G, Kavanagh PB, et al. Incremental prognostic value of post-stress left ventricular ejection fraction and volume by gated myocardial perfusion single photon emission computed tomography. *Circulation.* 1999;100:1035-1042.

20. Berman DS, Kang X, Slomka PJ, et al. Underestimation of extent of ischemia by gated SPECT myocardial perfusion imaging in patients with left main coronary artery disease. *J Nucl Cardiol.* 2007;14:521-528.

21. Wong SP, French JK, Lydon AM, et al. Relation of left ventricular sphericity to 10-year survival after acute myocardial infarction. *Am J Cardiol.* 2004;94:1270-1275.

22. Mannaerts HF, van der Heide JA, Kamp O, Stoel MG, Twisk J, Visser CA. Early identification of left ventricular remodelling after myocardial infarction. *Eur Heart J.* 2004;25:680-687.

23. Gibbons RJ, Lee KL, Cobb F, Jones RH. Ejection fraction response to exercise in patients with chest pain and normal coronary arteriograms. *Circulation.* 1981;64:952-957.

24. Abel RM, Reis RL. Effects of coronary blood flow and perfusion pressure on left ventricular contractility in dogs. *Circ Res.* 1970;27:961-971.

25. Dorbala S, Vangala D, Sampson U, Limaye A, Kwong R, Di Carli MF. Value of vasodilator left ventricular ejection fraction reserve in evaluating the magnitude of myocardium at risk and the extent of angiographic coronary artery disease: A 82Rb PET/CT study. *J Nucl Med.* 2007;48:349-358.

26. Bin J-P, Le E, Pelberg RA, Coggins MP, Wei K, Kaul S. Mechanism of inducible regional dysfunction during dipyridamole stress. *Circulation.* 2002;106:112-117.

27. Dilsizian V, Bacharach SL, Beanlands RS, et al. ASNC imaging guidelines/SNMMI procedure standard for positron emission tomography (PET) nuclear cardiology procedures. *J Nucl Cardiol.* 2016;23:1187-1226.

28. Otaki Y, Fish M, Miller RJ, Lemley M, Slomka P. Prognostic value of early left ventricular ejection fraction reserve during regadenoson stress solid-state SPECT-MPI. *J Nucl Cardiol.* 2020;Epub ahead of print.

TABLES

Table 1: Baseline Population Characteristics

	MACE occurred (n=2,120)	No MACE (n= 11,896)	*P*-value
Age (years), mean±SD	69.4±11.8	63.3±12.1	<0.001
Male, n(%)	1,471(69.4)	6,998(58.8)	<0.001
Body mass index(kg/m^2), mean±SD	28.1±5.7	28.4±6.3	0.263
Past medical history			
Hypertension, n(%)	1,593(75.1)	7,243(60.9)	<0.001
Diabetes, n(%)	810(38.2)	2,772(23.3)	<0.001
Dyslipidemia, n(%)	1,534(72.4)	7,219(60.7)	<0.001
Current smoker, n(%)	421(19.9)	2,712(22.8)	0.003
PVD, n(%)	462(21.8)	1,637(13.8)	<0.001
Prior MI, n(%)	549(25.9)	1,532(12.9)	<0.001
Prior revascularization, n(%)	1,088(47.6)	2,839(23.9)	<0.001
Family history of CAD, n(%)	451(21.3)	3,274(27.5)	<0.001
Typical angina, n(%)	159(7.5)	621(5.2)	<0.001
Resting vital signs, mean±SD			
Systolic BP (mmhg)	136.0±21.2	134.2±19.7	0.001
Diastolic BP (mmhg)	77.8±9.8	79.6±9.3	<0.001
Heart rate (bpm)	71.4±13.6	69.6±13.3	<0.001
Exercise stress, n(%)	523(24.7)	5,221(43.9)	<0.001

Table 1: Baseline population characteristics. BP – blood pressure, bpm – beats per minute, CAD – coronary artery disease, MACE – major adverse cardiovascular event, MI – myocardial infarction, PVD – peripheral vascular disease, SD – standard deviation.

Table 2: Imaging characteristics

	MACE Occurred (n=2,120)	No MACE (n= 11,896)	*P*-value
Rest shape index(%), mean±SD	64.9±8.3	63.9±7.5	<0.001
Stress shape index(%), mean±SD	65.5±8.4	63.1±7.1	<0.001
Post-stress change in Shape index(%), mean±SD	0.6±4.0	-0.8±4.1	<0.001
Rest eccentricity index(%), mean±SD	80.6±4.7	81.1±4.6	<0.001
Stress eccentricity index(%), mean±SD	80.2±5.0	81.3±4.5	<0.001
Post-stress change in eccentricity index(%), mean±SD	-0.4±3.0	0.3±2.8	<0.001
Resting TPD, mean±SD	3.8±7.7	1.6±4.9	<0.001
Stress TPD, mean±SD	8.2±9.6	4.3±6.6	<0.001
Ischemic TPD, mean±SD	4.4±4.0	2.7±3.0	<0.001
Resting LVEF, mean±SD	58.6±14.8	62.8±12.3	<0.001
Reduced LVEF (<40%), n(%)	251(11.8)	482(4.1)	<0.001
Stress LVEF, mean±SD	56.6±14.3	62.3±11.9	<0.001
Delta LVEF, mean±SD	-1.9±7.1	-0.5±7.2	<0.001
Resting LVEDV, mean±SD	82.4±45.5	70.7±33.7	<0.001
Stress LVEDV, mean±SD	84.0±46.4	70.2±34.5	<0.001
Delta LVEDV, mean±SD	1.6±12.6	-0.57±9.1	<0.001
Transient ischemic dilation, n(%)	101(4.8)	454(3.8)	0.046

Table 2: Imaging Characteristics. LVEDV – left ventricular end diastolic volume, LVEF – left ventricular ejection fraction, MACE – major adverse cardiovascular event, SD – standard deviation, TPD – total perfusion deficit.

Table 3: Univariable and Multivariable Associations with MACE

Variable	Adjusted HR (95% CI)	***P***-value
Rest shape index (per 10%)	1.05(0.94 – 1.17)	0.370
Post-stress change in shape index (per 10%)	1.38(1.20 – 1.58)	<0.001
Rest eccentricity index (per 10%)	0.97(0.81 – 1.17)	0.763
Post-stress change in eccentricity index (per 10%)	0.80(0.66 – 0.98)	0.033
Age	1.02(1.02 - 1.03)	<0.001
Male	1.23(1.11 - 1.36)	<0.001
Prior MI	1.19(1.06 – 1.34)	0.004
Prior PCI	1.69(1.53 – 1.87)	<0.001
Prior CABG	1.14(1.01 – 1.28)	0.037
Hypertension	1.15(1.05 - 1.26)	0.002
Diabetes	1.35(1.25 - 1.47)	<0.001
Pharmacologic stress	1.40(1.27 - 1.54)	<0.001
Typical angina	1.52(1.34 - 1.72)	<0.001
Ischemic ECG response	1.43(1.29 - 1.58)	<0.001
Resting TPD	1.01(1.00 - 1.01)	0.065
Ischemic TPD	1.12(1.11 - 1.13)	<0.001
Resting LVEF	0.99(0.99 - 0.99)	<0.001

Table 3. Adjusted Associations with major adverse cardiovascular events (MACE). Stress shape index and stress eccentricity index were not included in the multivariable model due to the inclusion of both rest and post-stress change in values. CABG – coronary artery bypass grafting, CAD – coronary artery disease, HR – hazard ratio, LVEF – left ventricular ejection fraction, MI – myocardial infarction, PCI – percutaneous coronary intervention, TPD – total perfusion deficit.

FIGURE LEGENDS

Figure 1

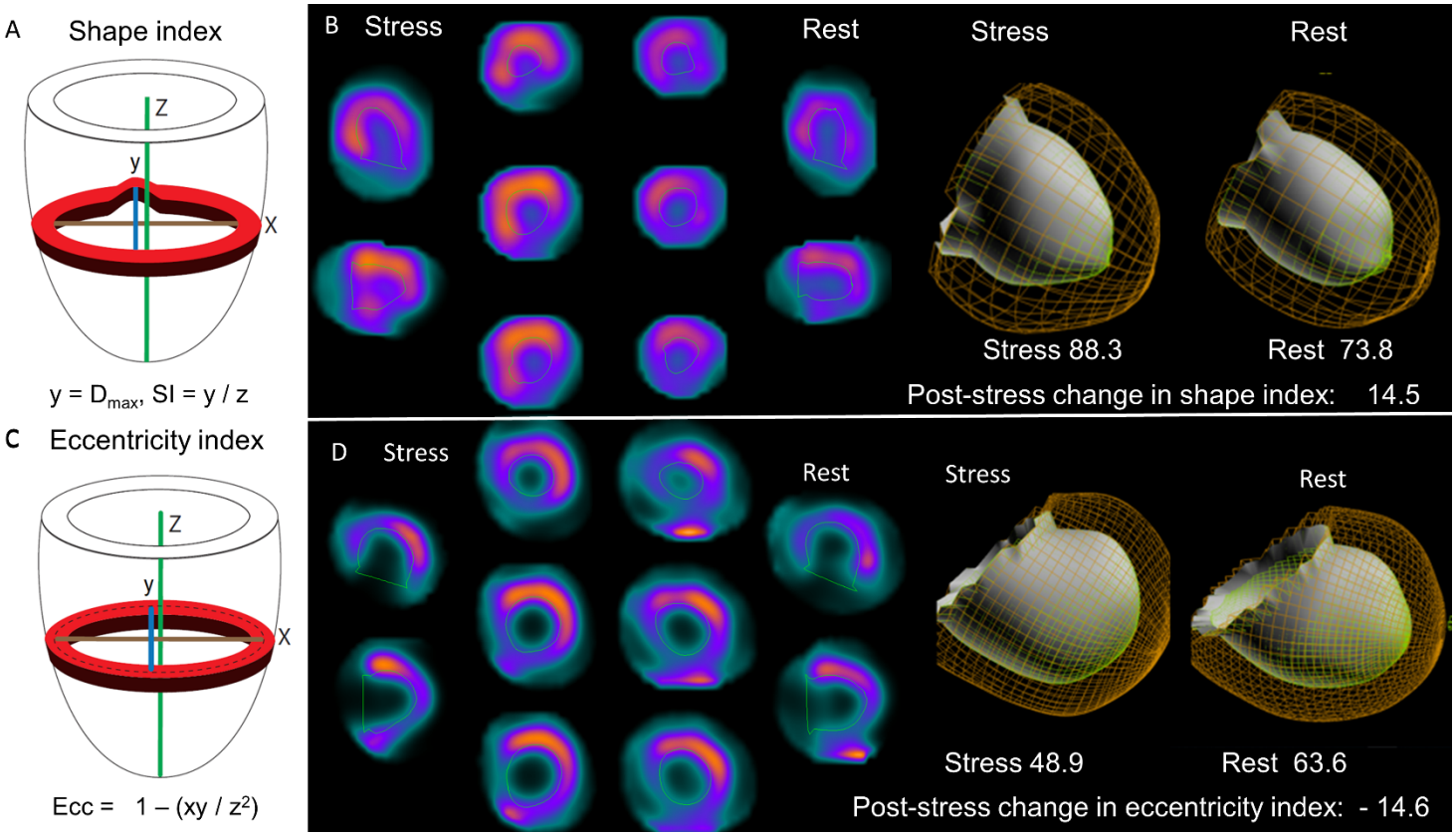

A) Shape index is calculated as the ratio of maximal short-axis diameter across all short-axis slices to the long-axis length, from apex to the mitral valve, using the endocardial surface. B) Patient with abnormal post-stress change in shape index, but normal post-stress change in eccentricity (0.3) who was admitted for unstable angina and underwent revascularization 231 days after SPECT MPI. C) Eccentricity index is calculated from the mid-myocardial surface of the fitted ellipsoid and does not account for regional anatomy. D) Patient with abnormal post-stress change in eccentricity index and mildly abnormal post-stress change in shape index (0.5), who died 290 days after SPECT MPI.

Figure 2

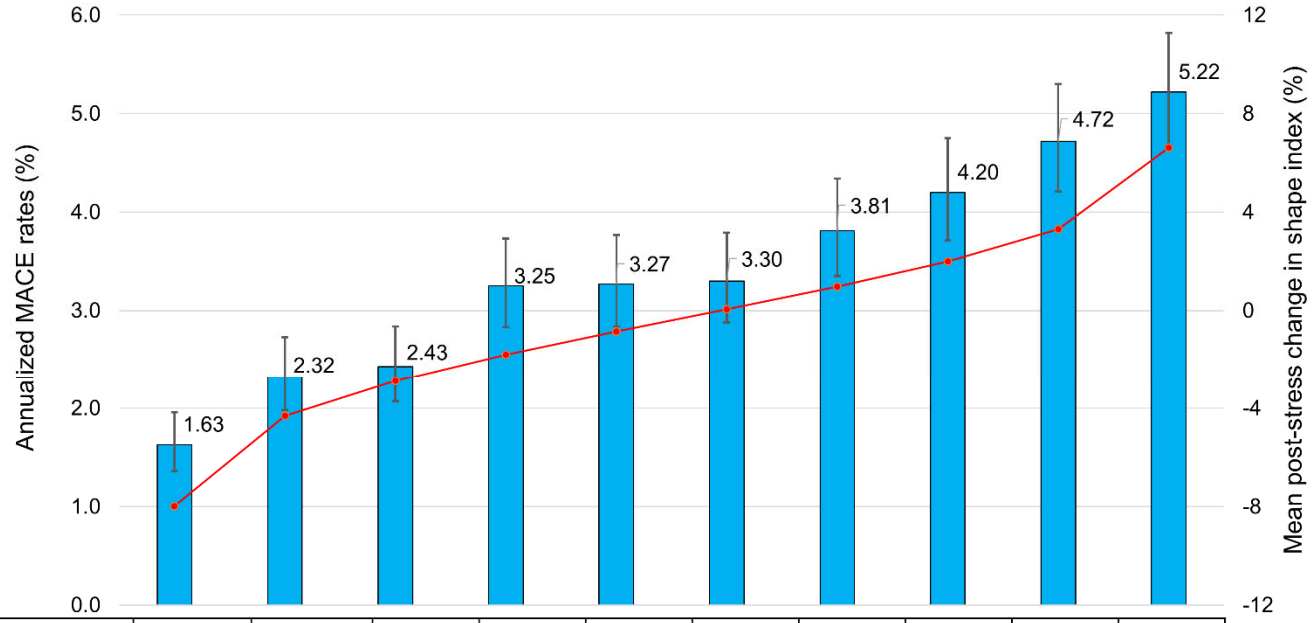

Decile	1st	2nd	3rd	4th	5th	6th	7th	8th	9th	10th
Mean	-7.99%	-4.31%	-2.88%	-1.79%	-0.85%	0.06%	0.97%	2.00%	3.31%	6.62%
N (MACE / total)	115 / 1402	149 / 1402	153 / 1401	200 / 1402	202 / 1401	204 / 1402	232 / 1402	254 / 1401	287 / 1402	324 / 1401

Annualized incidence of major adverse cardiovascular events (MACE) for deciles of post-stress change in shape index. The blue bars (with error bars showing 95% confidence interval) show annualized MACE rates. The values in the table reflect the total number of events during follow-up. The red line shows mean post-stress change in shape index for each decile, which the mean value also shown in the table.

Figure 3

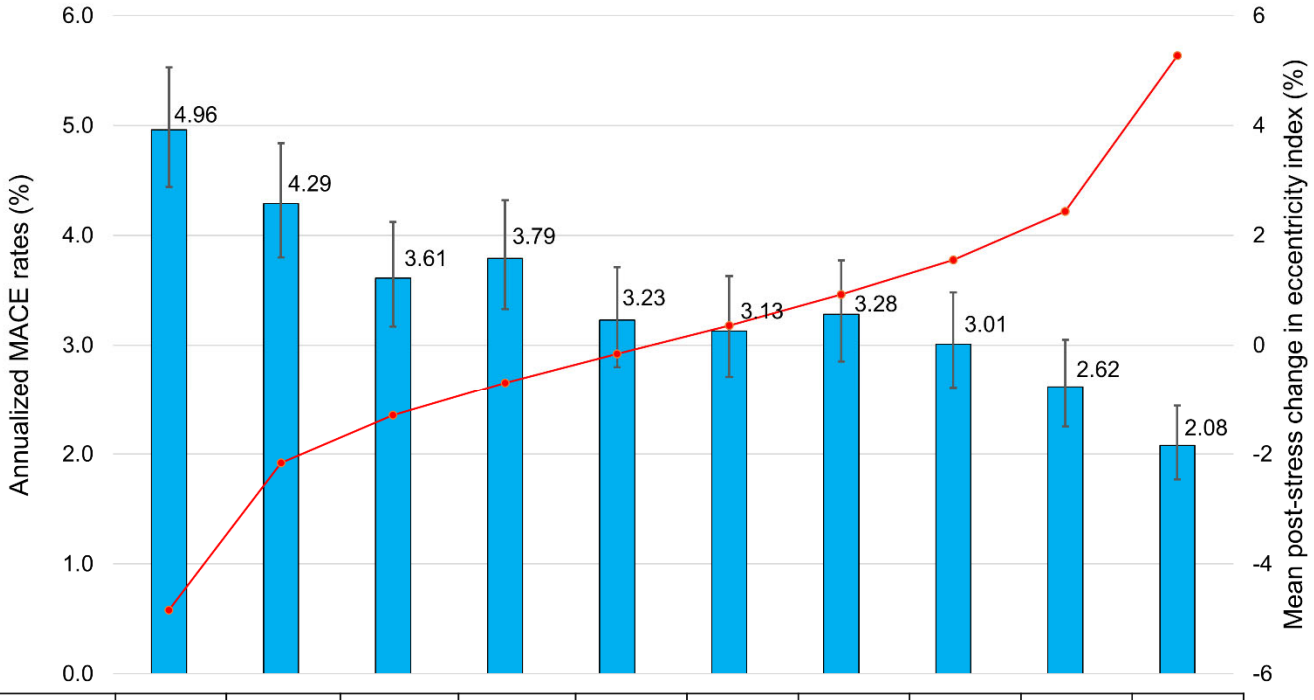

Decile	1st	2nd	3rd	4th	5th	6th	7th	8th	9th	10th
Mean	-4.84%	-2.16%	-1.29%	-0.69%	-0.16%	0.36%	0.92%	1.55%	2.44%	5.33%
N (MACE / total)	321 / 1402	262 / 1402	222 / 1401	227 / 1402	195 / 1401	193 / 1402	198 / 1402	185 / 1401	168 / 1402	149 / 1401

Annualized incidence of major adverse cardiovascular events (MACE) for deciles of change in eccentricity index. The blue bars (with error bars showing 95% confidence interval) show annualized MACE rates. The values in the table reflect the total number of events during follow-up. The red line shows mean post-stress delta eccentricity index for each decile, which the mean value also shown in the table.

Figure 4

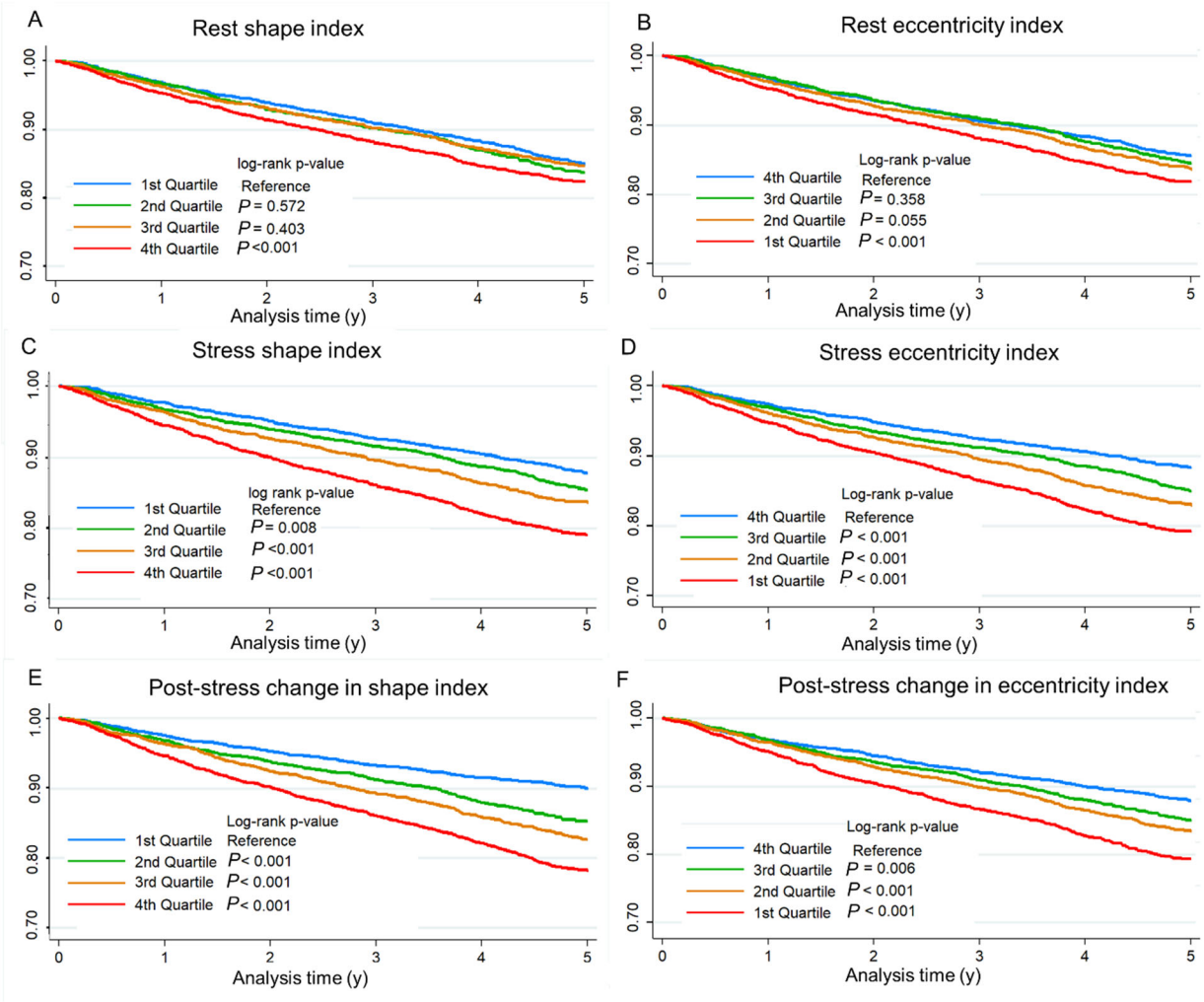

Kaplan-Meier survival curves for quartiles of rest, stress, and post-stress change in shape index (panels A, C, and E respectively) and eccentricity index (panels B, D, and F)

Graphical Abstract

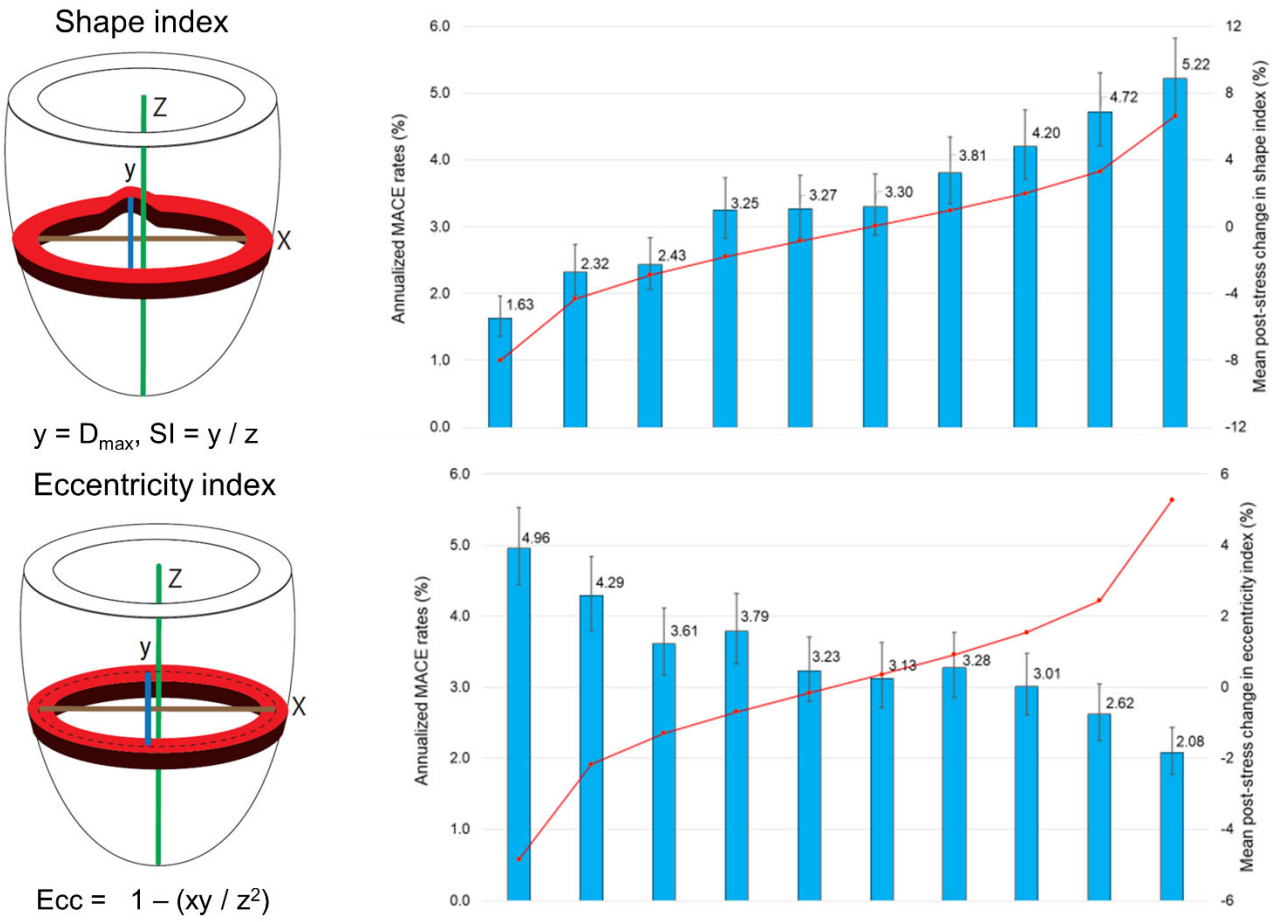

Supplemental Table 1:

	Pharmacologic stress (n=8,272)	Exercise stress (n=5,744)	P-value
Rest shape index(%), mean±SD	64.9 ± 8.0	63.1 ± 6.9	<0.001
Stress shape index(%), mean±SD	64.9 ± 7.8	61.4 ± 6.3	<0.001
Post-stress change in shape index(%), mean±SD	0.2 ± 4.1	-1.7 ± 3.9	<0.001
Rest eccentricity index(%), mean±SD	80.4 ± 4.7	81.9 ± 4.3	<0.001
Stress eccentricity index(%), mean±SD	80.3 ± 4.8	82.4 ± 3.9	<0.001
Post-stress change in eccentricity index(%), mean±SD	-0.1 ± 3.0	0.5 ± 2.6	<0.001
Resting TPD, mean±SD	2.4 ± 6.2	1.2 ± 4.2	<0.001
Stress TPD, mean±SD	5.7 ± 8.0	3.7 ± 5.8	<0.001
Ischemic TPD, mean±SD	3.2 ± 3.4	2.5 ± 3.0	<0.001
Resting LVEF, mean±SD	61.9 ± 14.0	62.5 ± 10.8	<0.001
Stress LVEF, mean±SD	60.8 ± 13.6	62.4 ± 10.4	0.003
Change in LVEF, mean±SD	-1.1 ± 7.3	-0.1 ± 7.2	<0.001
Resting LVEDV, mean±SD	73.7 ± 40.8	70.7 ± 27.5	<0.001
Stress LVEDV, mean±SD	75.5 ± 42.2	67.5 ± 26.8	<0.001
Change in LVEDV, mean±SD	1.8 ± 10.0	-3.2 ± 8.6	<0.001
Transient ischemic dilation, n(%)	353 (4.3)	202 (3.5)	0.046

Imaging Characteristics stratified by mode of stress. LVEDV – left ventricular end diastolic volume, LVEF – left ventricular ejection fraction, MACE – major adverse cardiovascular event, SD – standard deviation, TPD – total perfusion deficit

Supplemental Table 2: Unadjusted and Adjusted Associations with major adverse cardiovascular events (MACE) in a non-parsimonious model

Variable	Unadjusted HR (95% CI)	P-value	Adjusted HR (95% CI)	P-value
Rest shape index (per 10%)	1.16(1.09 – 1.22)	<0.001	1.06(0.95 – 1.18)	0.301
Stress shape index (per 10%)	1.40(1.33 – 1.47)	<0.001	*	*
Post-stress change in shape index (per 10%)	2.01(1.82 – 2.22)	<0.001	1.31(1.13 – 1.53)	<0.001
Rest eccentricity index (per 10%)	0.82(0.75 – 0.89)	<0.001	1.02(0.85 – 1.23)	0.828
Stress eccentricity index (per 10%)	0.63(0.58 – 0.69)	<0.001	*	*
Post-stress change in eccentricity index (per 10%)	0.52(0.46 – 0.59)	<0.001	0.81(0.66 – 0.99)	0.041
Age (per 10 years)	1.52(1.47 – 1.58)	<0.001	1.31(1.26 – 1.37)	<0.001
Male	1.62(1.48 – 1.78)	<0.001	1.25(1.12 – 1.40)	<0.001
Body mass index	0.98(0.97 – 0.99)	<0.001	0.98(0.97 – 0.99)	0.002
Hypertension	1.82(1.65 – 2.01)	<0.001	1.20(1.07 – 1.33)	0.001
Diabetes	1.87(1.72 – 2.04)	<0.001	1.37(1.25 – 1.51)	<0.001
Dyslipidemia	1.64(1.49 – 1.81)	<0.001	1.02(0.92 – 1.13)	0.676
Current smoker	0.95(0.83 – 1.06)	0.385	1.00(0.89 – 1.12)	0.975
PVD	1.82(1.63 – 2.01)	<0.001	1.05(0.94 – 1.18)	0.399
Prior MI	2.40(2.18 – 2.65)	<0.001	1.20(1.07 – 1.36)	0.002
Prior revascularization	2.87(2.63 – 3.12)	<0.001	1.61(1.45 – 1.79)	<0.001
Family history of CAD	0.73(0.66 – 0.82)	<0.001	0.90(0.81 – 1.00)	0.047
Typical angina	1.37(1.16 – 1.61)	<0.001	1.20(1.02 – 1.41)	0.031

Systolic BP (per 10 mmhg)	1.04(1.02 – 1.07)	<0.001	1.05(1.02 – 1.08)	<0.001
Diastolic BP (per 10 mmhg)	0.85(0.82 – 0.89)	<0.001	0.84(0.80 – 0.89)	<0.001
Heart Rate (per 10 bpm)	1.07(1.04 – 1.10)	<0.001	1.14(1.10 – 1.17)	<0.001
Exercise stress	0.44(0.40 – 0.48)	<0.001	0.66(0.60 – 0.74)	<0.001
Resting TPD	1.05(1.04 – 1.05)	<0.001	0.99(0.99 – 1.00)	0.086
Stress TPD	1.05(1.04 – 1.05)	<0.001	*	*
Ischemic TPD	1.12(1.11 – 1.13)	<0.001	1.05(1.03 – 1.06)	<0.001
Resting LVEF	0.97(0.97 – 0.98)	<0.001	0.99(0.98 – 0.99)	<0.001
Stress LVEF	0.97(0.96 – 0.97)	<0.001	*	*
Change in LVEF	0.98(0.97 – 0.99)	<0.001	0.98(0.98 – 0.99)	<0.001
Resting LVEDV	1.01(1.01 – 1.01)	<0.001	1.00(0.99 – 1.00)	0.199
Stress LVEDV†	1.01(1.01 – 1.01)	<0.001	*	*
Change in LVEDV†	1.02(1.02 – 1.02)	<0.001	1.00(1.00 – 1.00)	0.639
Transient ischemic dilation	1.23(1.01 – 1.50)	0.043	0.90(0.73 – 1.11)	0.328

Unadjusted and Adjusted Associations with major adverse cardiovascular events (MACE) in a non-parsimonious model. *- variable excluded due to inclusion of rest and change in variables. †Multivariable results similar when considering left ventricular end-systolic volume in place of left ventricular end-diastolic volume (LVEDV). CAD – coronary artery disease, HR – hazard ratio, LVEDV – left ventricular end-diastolic volume, LVEF – left ventricular ejection fraction, MI – myocardial infarction, PVD – peripheral vascular disease, TID – transient ischemic dilation.

Supplemental Table 3: Summary of Reclassification

Variable	Event reclassification	Non-event reclassification	Continuous net reclassification
Rest shape index	-0.057 (-0.085 – 0.081)	0.044 (-0.032 – 0.066)	-0.013 (-0.065 – 0.061)
Stress shape index	-0.014 (-0.044 – 0.021)	0.093 (0.066 – 0.116)	0.079 (0.028 – 0.130)
Post-stress change in Shape Index	0.080 (0.051 – 0.118)	0.074 (0.048 – 0.098)	0.154 (0.108 – 0.209)
Rest eccentricity index	-0.056 (-0.082 – 0.094)	0.037 (-0.089 – 0.116)	-0.018 (-0.069 – 0.076)
Stress eccentricity index	-0.066 (-0.093 to -0.024)	0.127 (0.104 – 0.150)	0.061 (0.016 – 0.116)
Post-stress change in eccentricity index	0.061 (0.028 – 0.098)	0.056 (0.027 – 0.087)	0.117 (0.069 – 0.174)

Summary of Reclassification for inclusion of shape index and eccentricity variables. Multivariable models adjusted for all variables other than shape index and eccentricity outlined in Table 3 including stress and ischemic TPD.

Supplemental Table 4: Comparison of Prognostic Accuracy

Variable	Threshold method	Abnormal threshold	Annualized MACE abnormal	Annualized MACE normal	PPV	NPV
Rest shape index	ROC	>64.21	3.6%	3.2%	16.2%	85.8%
	95th Percentile	>77.07	4.7%	3.3%	21.5%	85.2%
Stress shape index	ROC	>63.83	4.2%	2.7%	18.5%	87.5%
	95th Percentile	>76.62	6.1%	3.2%	27.1%	85.5%
Post-stress change in shape index	ROC	>0.236	4.5%	2.6%	19.5%	88.0%
	95th Percentile	>5.65	5.0%	3.3%	23.3%	85.3%
Rest eccentricity index	ROC	<81.47	3.1%	3.7%	16.4%	86.1%
	95th Percentile	<72.63	3.8%	3.4%	18.1%	85.0%
Stress eccentricity index	ROC	<81.32	4.1%	2.8%	18.1%	87.4%
	95th Percentile	<73.04	5.6%	3.3%	24.8%	85.4%
Post-stress change in eccentricity index	ROC	< -0.18	4.1%	2.8%	18.1%	87.2%
	95th Percentile	< -3.97	4.7%	3.2%	22.5%	85.3%

Comparison of prognostic accuracy for abnormal thresholds derived using the Youden index from receiver-operating characteristic (ROC) curves or as the 95th percentile. MACE – major adverse cardiovascular events, NPV – negative predictive value, PPV – positive predictive value.

Supplemental Table 5: Thresholds for Abnormal Change in Shape Index

	ROC AUC (95% CI)	Abnormal threshold	Annualized MACE negative	Annualized MACE positive
Overall	0.597 (0.584 – 0.610)	>0.236	2.6%	4.5%
Site held out				
Assuta	0.620 (0.603 – 0.637)	>0.263	4.4%	5.3%
BW	0.597 (0.584 – 0.610)	>0.236	0.6%	3.7%
CSMC	0.592 (0.577 – 0.607)	>0.236	2.4%	4.1%
Oregon	0.587 (0.572 – 0.601)	>0.236	1.8%	4.7%
Ottawa	0.587 (0.573 – 0.6010	>0.358	2.0%	3.3%

Thresholds for abnormal change in shape index in the overall population and in a leave one site out approach. In the leave one site out approach, receiver-operating characteristic (ROC) curves were generated from the remaining sites and the optimal ROC thresholds were then tested in the held-out site. AUC – area under the curve, BW – Brigham and Women's, CI – confidence interval, CSMC – Cedars-Sinai Medical Center, MACE – major adverse cardiovascular event.

Supplemental Table 6:

	Unadjusted HR (95% CI)	p-value	Adjusted HR (95% CI)	P-value
Rest shape index	1.31 (1.23 – 1.40)	<0.001	1.27 (1.12 – 1.45)	<0.001
Stress shape index	1.58 (1.49 – 1.67)	<0.001	*	*
Post-stress change in Shape Index	2.18 (1.93 – 2.46)	<0.001	1.59 (1.34 – 1.88)	<0.001
Rest eccentricity index	0.65 (0.59 – 0.72)	<0.001	1.09 (0.87 – 1.36)	0.455
Stress eccentricity index	0.52 (0.47 – 0.57)	<0.001	*	*
Post-stress change in eccentricity index	0.53 (0.45 – 0.62)	<0.001	1.05 (0.82 – 1.34)	0.713

Associations with all-cause mortality. Multivariable model included the same variables outlined in Table 3. *- variable excluded due to inclusion of rest and change in variables. HR – hazard ratio

Supplemental Table 7:

	Mean ± SD	Unadjusted HR (95% CI)	p-value	Adjusted HR (95% CI)	P-value
Exercise stress (n=5,744)					
Rest shape index	63.1 ± 6.9	0.90 (0.80 – 1.02)	0.095	0.74 (0.55 – 0.98)	0.036
Stress shape index	61.4 ± 6.3	1.19 (1.04 – 1.36)	0.009	*	*
Post-stress change in shape index	-1.7 ± 3.9	2.31 (1.85 – 2.90)	<0.001	1.14 (0.80 – 1.63)	0.477
Rest eccentricity index	81.9 ± 4.3	1.07 (0.88 – 1.30)	0.520	0.57 (0.36 – 0.92)	0.022
Stress eccentricity index	82.4 ± 3.9	0.74 (0.60 – 0.90)	0.003	*	*
Post-stress change in Eccentricity Index	0.5 ± 2.6	0.40 (0.29 – 0.56)	<0.001	0.44 (0.25 – 0.77)	0.004
Pharmacologic stress (n=8,272)					
Rest shape index	64.7 ± 8.0	1.16 (1.10 – 1.23)	<0.001	1.14 (1.01 – 1.27)	0.030
Stress shape index	64.9 ± 7.8	1.29 (1.22 – 1.36)	<0.001	*	*
Post-stress change in shape index	0.2 ± 4.1	1.53 (1.36 – 1.72)	<0.001	1.41 (1.22 – 1.63)	<0.001
Rest eccentricity index	80.4 ± 4.7	0.87 (0.79 – 0.96)	0.007	1.08 (0.89 – 1.31)	0.437
Stress eccentricity index	80.3 ± 4.8	0.74 (0.67 – 0.81)	<0.001	*	*
Post-stress change in eccentricity index	-0.1 ± 3.0	0.65 (0.56 – 0.75)	<0.001	0.90 (0.73 – 1.11)	0.329

Associations between shape index and eccentricity index in patients undergoing exercise stress and pharmacologic stress. Mean of all parameters was significantly different between exercise and pharmacologic stress. Multivariable models are the same as outlined for Table 3. Formal interaction testing was not significant for change in shape index (p=0.066) or change in eccentricity index (p=0.119). *- variable excluded due to inclusion of rest and change in variables.

Supplemental Table 8:

	Mean ± SD	Unadjusted HR (95% CI)	p-value	Adjusted HR (95% CI)	P-value
Preserved LVEF (≥40%) (n=13,283)					
Rest shape index	63.7 ± 7.4	1.07 (1.01 – 1.14)	0.019	1.01 (0.89 – 1.13)	0.928
Stress shape index	63.1 ± 7.2	1.32 (1.25 – 1.40)	<0.001	*	*
Post-stress change in shape index	-0.6 ± 4.1	2.03 (1.83 – 2.26)	<0.001	1.35 (1.16 – 1.57)	<0.001
Rest eccentricity index	81.2 ± 4.5	0.89 (0.81 – 0.98)	0.015	0.90 (0.74 – 1.10)	0.322
Stress eccentricity index	81.3 ± 4.5	0.67 (0.61 – 0.73)	<0.001	*	*
Post-stress change in eccentricity index	0.2 ± 2.8	0.50 (0.44 – 0.58)	<0.001	0.73 (0.59 – 0.90)	0.004
Reduced LVEF (<40%) (n=733)					
Rest shape index	69.4 ± 8.7	1.14 (0.99 – 1.31)	0.065	1.39 (1.07 – 1.81)	0.014
Stress shape index	69.9 ± 8.8	1.22 (1.07 – 1.40)	0.003	*	*
Post-stress change in shape index	0.5 ± 4.5	1.35 (1.05 – 1.73)	0.020	1.66 (1.18 – 2.34)	0.004
Rest eccentricity index	78.2 ± 5.3	0.91 (0.73 – 1.14)	0.402	1.69 (1.07 – 2.66)	0.024
Stress eccentricity index	78.1 ± 5.1	0.86 (0.68 – 1.08)	0.186	*	*
Post-stress change in eccentricity index	-0.2 ± 3.3	0.86 (0.59 – 1.25)	0.436	1.61 (0.92 – 2.81)	0.093

Associations between shape index and eccentricity index in patients with preserved or reduced LVEF. Mean of all parameters was significantly different between reduced and preserved LVEF. Multivariable models are the same as outlined for Table 3. Interaction testing was not significant for post-stress change in shape index (p=0.279) or post-stress change in eccentricity index (p=0.084). *- variable excluded due to inclusion of rest and post-stress change in variables.

Supplemental Table 9:

	Mean ± SD	Unadjusted HR (95% CI)	p-value	Adjusted HR (95% CI)	P-value
DSPECT (n=5,660)					
Rest shape index	64.7 ± 8.6	1.23 (1.14 – 1.34)	<0.001	1.20 (1.05 – 1.37)	0.006
Stress shape index	63.9 ± 8.3	1.41 (1.32 – 1.50)	<0.001	*	*
Post-stress change in shape index	-0.7 ± 4.9	1.88 (1.60 – 2.21)	<0.001	1.61 (1.36 – 1.91)	<0.001
Rest eccentricity index	80.7 ± 5.3	0.73 (0.63 – 0.83)	<0.001	1.19 (0.94 – 1.50)	0.153
Stress eccentricity index	81.0 ± 5.1	0.59 (0.52 – 0.67)	<0.001	*	*
Post-stress change in eccentricity index	0.3 ± 3.8	0.39 (0.30 – 0.51)	<0.001	0.96 (0.76 – 1.22)	0.761
GE530 (n=8,356)					
Rest shape index	63.6 ± 6.9	1.13 (1.05 – 1.22)	0.001	0.95 (0.80 – 1.12)	0.530
Stress shape index	63.2 ± 6.7	1.43 (1.33 – 1.55)	<0.001	*	*
Post-stress change in shape index	-0.4 ± 3.5	2.11 (1.86 – 2.40)	0.020	1.24 (1.00 – 1.53)	0.049
Rest eccentricity index	81.2 ± 4.1	0.86 (0.76 – 0.96)	0.009	0.74 (0.56 – 0.97)	0.031
Stress eccentricity index	81.3 ± 4.1	0.64 (0.57 – 0.71)	0.186	*	*
Post-stress change in eccentricity index	0.1 ± 2.0	0.55 (0.47 – 0.64)	0.436	0.65 (0.46 – 0.93)	0.017

Associations between shape index and eccentricity index in patients imaged with DSPECT or GE530 cameras. Multivariable models are the same as outlined for Table 3. Interaction testing was not significant for post-stress change in shape index (p=0.113) or post-stress change in eccentricity index (p=0.687). *- variable excluded due to inclusion of rest and post-stress change in variables.

Supplemental Figure 1: Correlation between shape index and eccentricity index

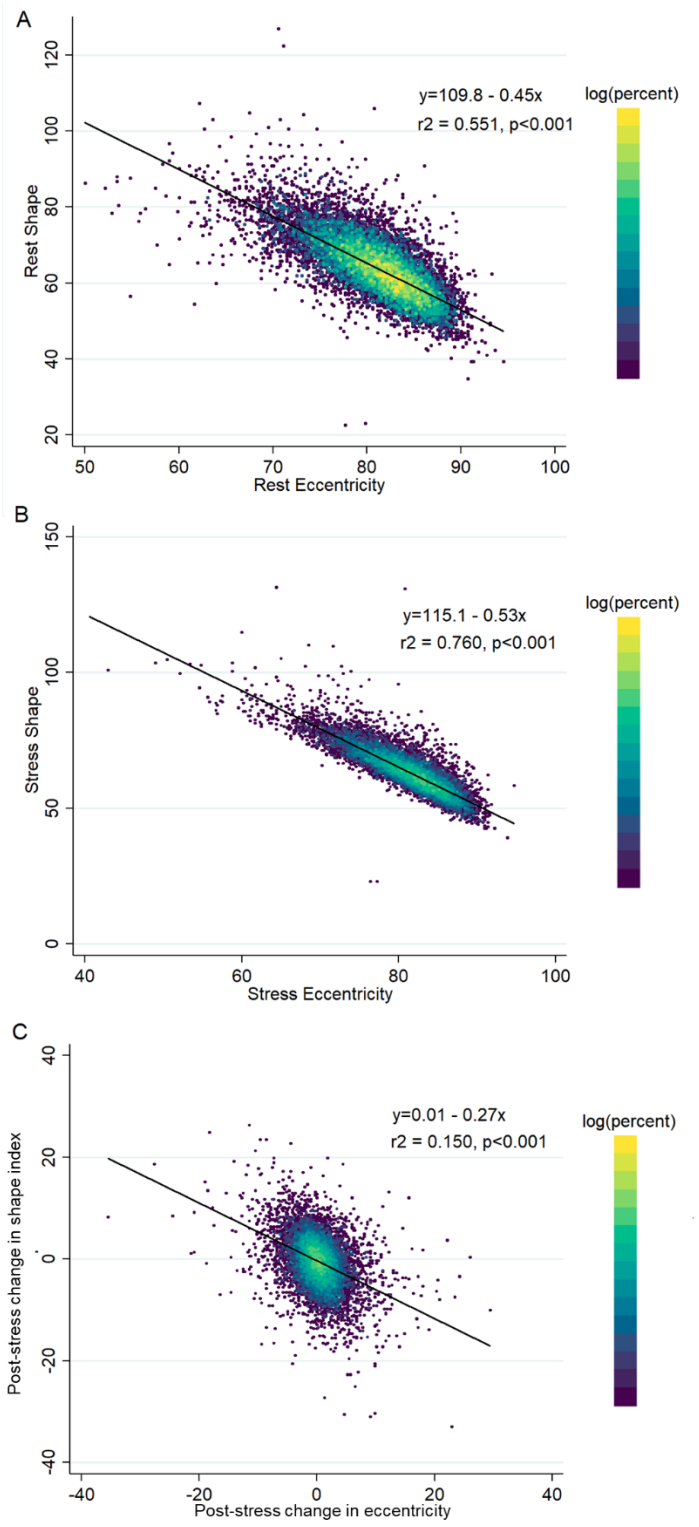

Supplemental Figure 1: Correlation gradient plots between shape index and eccentricity index. Rest (A), stress (B) and post-stress change in (C) values were all significantly correlated ($p<0.001$).

Supplemental Figure 2 Correlation gradient plots between change in shape index and eccentricity index with transient ischemic dilation ratio and change in left ventricular ejection fraction

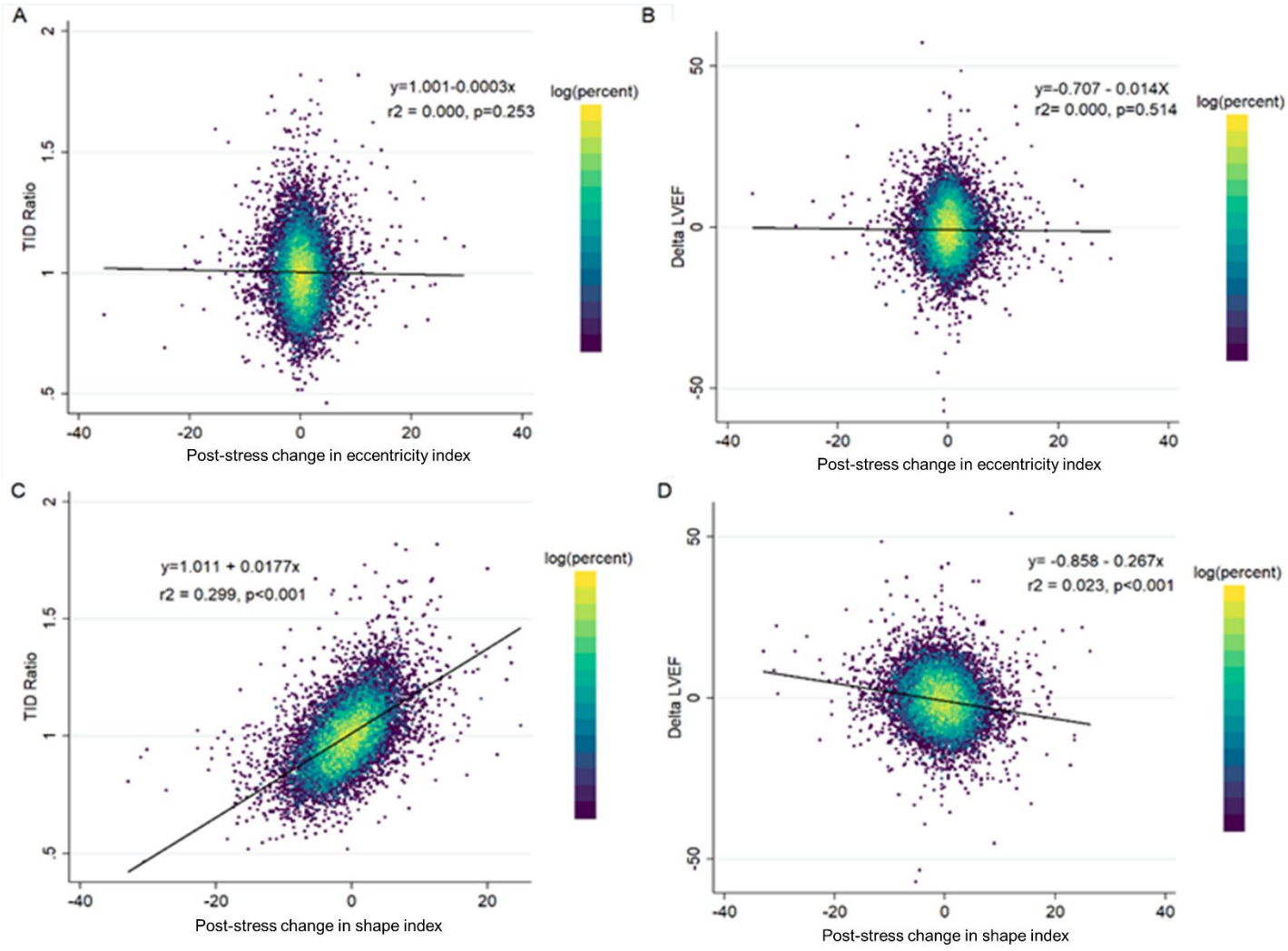

Correlation gradient plots between post-stress change in shape index and eccentricity index with transient ischemic dilation (TID) ratio and post-stress change in left ventricular ejection fraction (LVEF). There was no correlation between post-stress change in eccentricity index and TID (A) or change in LVEF (B). There was poor correlation between post-stress change in shape index and TID (C) and post-stress change in LVEF (D).

Supplemental Figure 3: Correlation between Shape Index and Eccentricity Index with Left Ventricular Ejection Fraction.

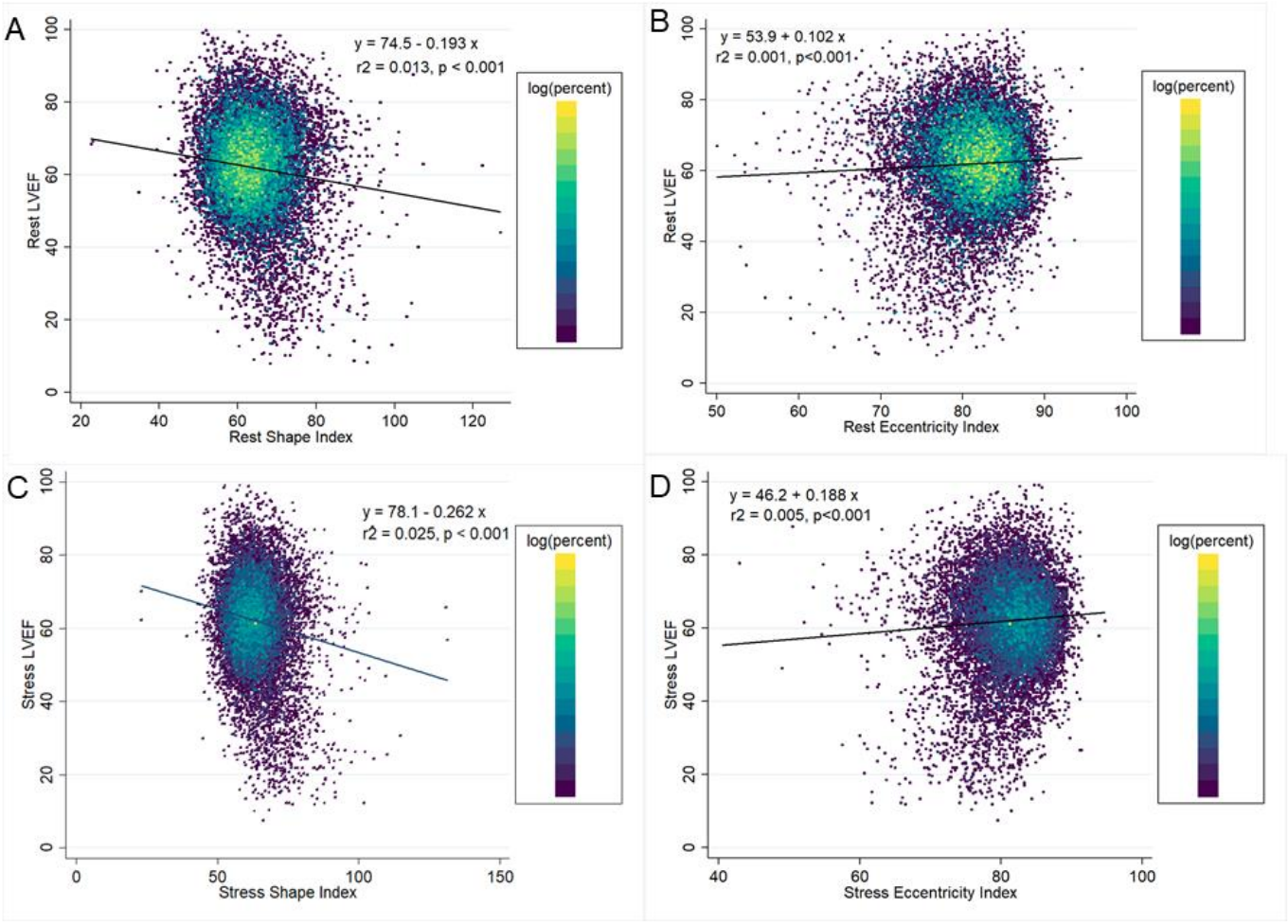

Correlation between shape index and eccentricity index with left ventricular ejection fraction (LVEF). Correlation shown for rest LVEF and rest shape index (panel A), rest LVEF and rest eccentricity index (panel B), stress LVEF and stress shape index (panel C), and stress LVEF and stress eccentricity index (panel D).

Supplemental Figure 4:

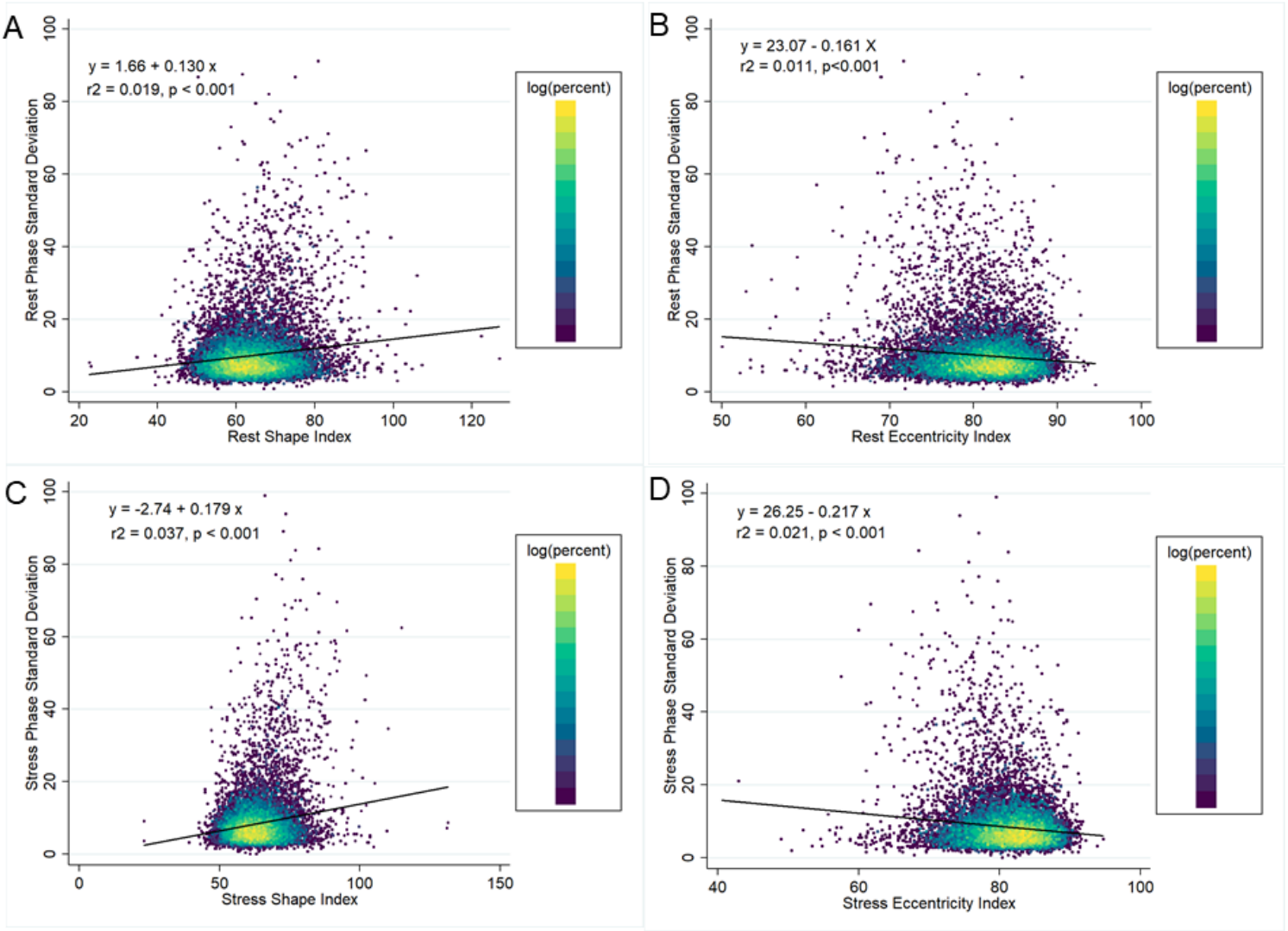

Correlation between Shape Index and Eccentricity Index with phase standard deviation (SD). Correlation shown for rest phase SD and rest shape index (panel A), rest phase SD and rest eccentricity index (panel B), stress phase SD and stress shape index (panel C), and stress phase SD and stress eccentricity index (panel D).

Supplemental Figure 5: Comparison of area under the curve for eccentricity index and shape index variables

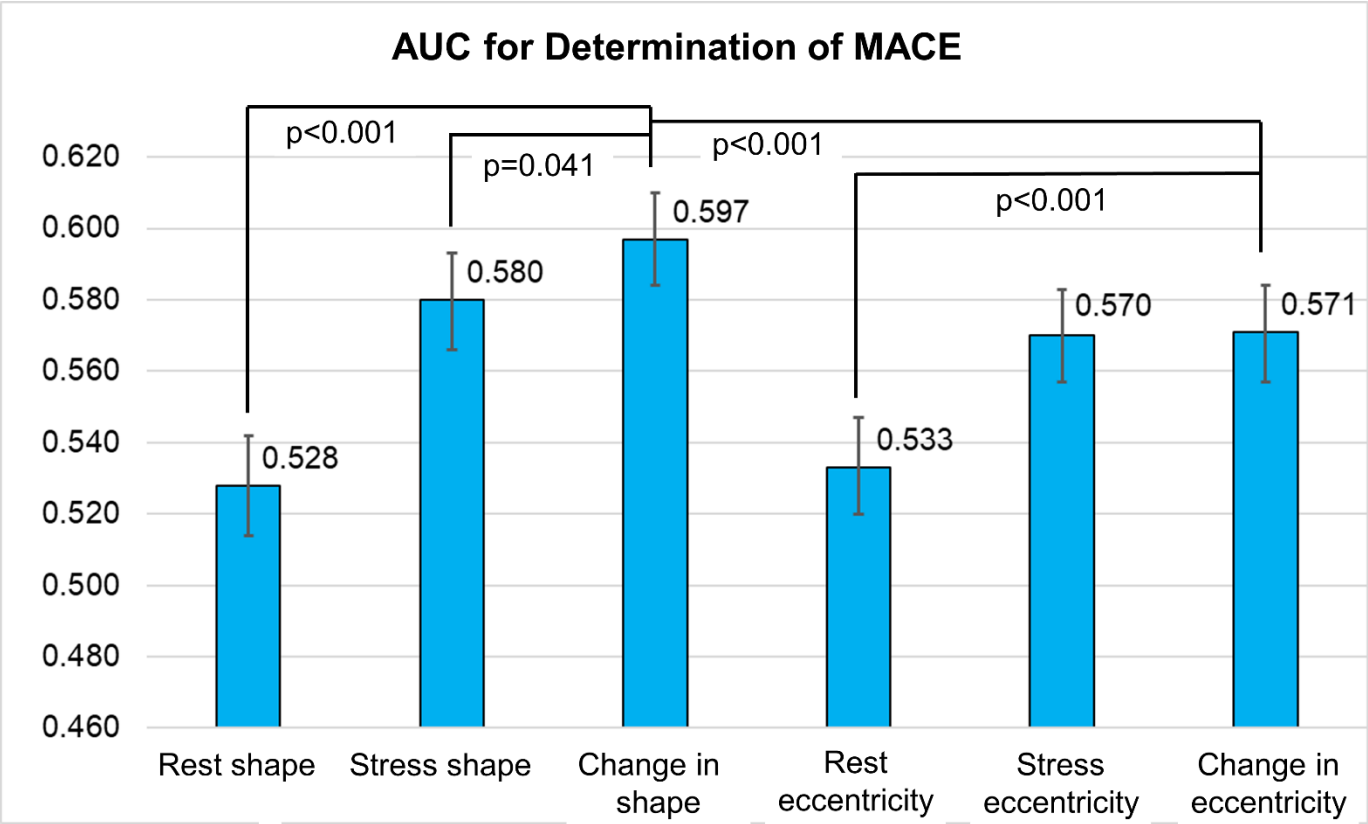

Comparison of receiver operating characteristic (ROC) area under the curve (AUC) of eccentricity index and shape index variables for MACE. Post-stress change in shape index had significantly higher AUC compared to all other measures. There was no significant difference in discrimination between stress eccentricity index and post-stress change in eccentricity index.

MACE – major adverse cardiovascular event.